STABILIZATION OF AERODYNAMICALLY EXCITED TURBOMACHINERY WITH HYDRODYNAMIC JOURNAL BEARINGS AND SUPPORTS*

Lloyd E. Barrett and Edgar J. Gunter
Department of Mechanical and Aerospace Engineering
University of Virginia
Charlottesville, Virginia 22903

SUMMARY

A method of analyzing the first mode stability and unbalance response of multimass flexible rotors is presented whereby the multimass system is modeled as an equivalent single mass modal model including the effects of rotor flexibility, general linearized hydrodynamic journal bearings, squeeze film bearing supports and rotor aerodynamic cross coupling. Expressions for optimum bearing and support damping are presented for both stability and unbalance response. The method is intended to be used as a preliminary design tool to quickly ascertain the effects of bearing and support changes on rotor-bearing system performance.

INTRODUCTION

The purpose of this paper is to present a method that is easily applied to a large class of industrial turbomachines which will predict the instability onset speeds including the effects of shaft flexibility, generalized hydrodynamic journal bearings, squeeze film bearing supports and aerodynamic rotor excitation. By restricting the analysis to the class of turbomachines which have their mass centers inboard of the bearings and are relatively symmetric about the mass center, a simplified rotor model is established that allows the equations of motion to be manipulated analytically. The restriction to turbomachines of this class does not severely limit its usefulness or applicability since the majority of industrial machines fall within this class. A major advantage of the method is that it allows machine designers to quickly determine the effects of bearing changes, shaft modifications and bearing support designs to determine appropriate system designs. Those designs deemed appropriate using the method can be further verified and finalized using more general analysis tools. A large time and cost savings should be realized by using the method to eliminate impractical designs without incurring the high computer costs and large amounts of data reduction time required using more general rotor dynamic analysis programs. The method is intended to supplement the more general techniques, not to replace them.

* This work was supported in part by the U.S. Army Research Office, Grant No. DAG 29-77-C-0009, NASA Lewis Research Center, Grant No. NSG-3105, Dept. of Energy, Grant No. EF-76-5-01-2479, and the Industrial Research Program, University of Virginia.

Specifically the method represents the rotor, bearings and supports as a linear dynamical system with the rotor represented by a generalized modal mass and modal stiffness. The inclusion of aerodynamic effects using the Alford model shows that an optimum bearing or support damping exists which will maximize the aerodynamic forces required to produce rotor instability for a given rotor and bearing or support flexibility. Definite expressions for the optimum damping are derived which eliminates the requirement of a parametric variation to find the optimum damping.

A number of instability mechanisms have been identified over the years. Chief among these are hydrodynamic bearings and aerodynamic effects.

(1) Hydrodynamic journal bearings - Most industrial turbomachine rotors are supported in fluid film bearings. Bearings with fixed geometries develop forces within the lubricant film which couple the motion of the rotor in any two orthogonal transverse directions and can produce instability under certain conditions of rotor speed and bearing load. Recent emphasis has been placed on determining the linearized fluid film force coefficients for various bearing geometries which can be used for linear stability analyses (refs. 1-9).

(2) Interaction with working fluid flow (Aerodynamic cross coupling) - The vibratory motion of a rotor within the machine working fluid can produce differential pressures around the rotor which result in destabilizing forces and moments. Because of the very complicated nature of the flows around turbine blades and through centrifugal impeller passages a general analysis describing the working fluid forces as a function of rotor motion has not been developed. The coupling between the working fluid and the rotor is commonly referred to as aerodynamic cross coupling.

The most commonly used approximation for predicting the magnitude of aerodynamic cross coupling assumes that the radial deflection of the rotor produces a variation in the thermodynamic efficiency around the impeller circumference and hence a torque variation (ref. 10). The differential torque produces a force on the impeller proportional to the displacement and perpendicular to it in the direction of impeller rotation and thus tends to drive the rotor in a forward (same direction as rotation) whirl. The cross coupling force on each impeller is a function of stage mean torque, pitch radius of the impeller, blade length and impeller displacement. A damping force is not postulated. The force is also proportional to a generally unknown constant which is a function of fluid mass flow rate, pressure, enthalpy and other fluid properties (ref. 10).

Figure 1 shows the frequency spectra for a 7-stage industrial centrifugal compressor designed to operate at 13500 rpm. Originally mounted in rigidly supported tilting pad bearings, the machine became unstable when the rotor speed exceeded 10500 rpm. The instability was due to aerodynamic cross coupling and seal forces. The spectra in figure 1a illustrates the subsynchronous frequency representing the instability shown by the 4300 cpm component of the spectra. This frequency was identified as the first damped frequency of the system and remained nearly constant as the machine speed was increased. The synchronous unbalance excitation is indicated by the 1N line and is seen to peak at about 4300 rpm. The vibration at the subsynchronous frequency was

sufficiently large to pervent sustained operation at 13500 rpm and the machine operation was restricted to below 10000 rpm for a considerable period of time. Monetary losses to the user due to reduced production capability were large.

Figure 1b shows the spectra after installation of properly designed squeeze bearings at the tilting pad bearing locations. The subsynchronous instability has been entirely eliminated. The unit has been successfully operated at full production capability for nearly four years with no indication of instability (ref. 11).

SYMBOLS

a	Constant
c	Bearing radial clearance, L
c_b	Tilting pad bearing assembled radial clearance, L
c_{ij}	Damping coefficient for i^{th} direction due to velocity in j^{th} direction, FTL^{-1}
c_p	Tilting pad bearing pad ground in clearance, L
c_r	Average radial damping coefficient, $(c_{ii} + c_{jj})/2$, FTL^{-1}
c_{ro}	Optimum average radial damping coefficient, FTL^{-1}
C_{ij}	$c_{ij}(2c\omega/W)$, dim.
C_o	$c_o(2c\omega/W)$, dim.
C_r	$c_r(2c\omega/W)$, dim.
C_{ro}	$c_{ro}(2c\omega/W)$, dim.
D	Bearing diameter, L
D_1	Defined by equation (19), dim.
D_2	Defined by equation (20), dim.
k_i	Modal stiffness for i^{th} mode, FL^{-1}
k_{ij}	Stiffness coefficient for force in i^{th} direction due to displacement in j^{th} direction, FL^{-1}
k_r	Average radial bearing stiffness $(k_{ii} + k_{jj})/2$, FL^{-1}
k_{rs}	Squeeze film bearing retainer spring stiffness, FL^{-1}
k_s	Fundamental shaft modal stiffness, FL^{-1}

K	Ratio of total bearing principal stiffness to shaft stiffness, dim.
K_c	Average cross coupled bearing stiffness, dim.
K_{ij}	$k_{ij}(c/W)$, dim.
K_r	$k_r(c/W)$, dim.
m	Mass, FT^2L^{-1}
N	Rotor speed, rpm
N_{cr}	Rigid bearing rotor critical speed, rpm
p	real part of eigenvalue, T^{-1}
P	p/ω_d, dim.
q	Aerodynamic cross coupling, FL^{-1}
Q	$2cq/W$, dim.
Q_m	Maximum value of Q, dim.
R	Bearing radius, L
s	Complex eigenvalue, T^{-1}
t	Time, T^{-1}
T	ωt, dim.
W	Weight, F
W_T	Total rotor weight, F
W_m	Rotor modal weight, F
x	Displacement in x-direction, L
X	x/c, dim.
$\{x\}$	Vector of x displacements, L
y	Displacement in y-direction, L
Y	y/c, dim.
$\bar{\delta}$	W/ck_s, dim.
λ	Imaginary part of eigenvalue, ω_d/ω, dim.

ω Rotor speed, T^{-1}

ω_{cr} Rotor rigid bearing critical speed, T^{-1}

ω_d Damped natural frequency, T^{-1}

ω_o Rotor operating speed, T^{-1}

ω_s Rotor instability onset speed, T^{-1}

ω_{sr} Rigid rotor instability onset speed, T^{-1}

Ω $\omega\sqrt{c/g}$, dim.

Ω_o $\omega_o\sqrt{c/g}$, dim.

Ω_s $\omega_s\sqrt{c/g}$, dim.

Ω_{sr} $\omega_{sr}\sqrt{c/g}$, dim.

ANALYSIS

Equations of Motion

Consider the generic rotor-bearing system shown schematically in figure 2. This system is representative of a large class of rotors supported in two bearings with most of the mass between the bearings. These machines generally operate above the first critical speed and the instability that occurs is generally associated with the first mode of the system (ref.12). The homogeneous equations of motion for the system are

$$m\ddot{x}_2 + k_s(x_2 - x_1) + q\,y_2 = 0 \tag{1}$$

$$m\ddot{y}_2 + k_s(y_2 - y_1) - q\,x_2 = 0 \tag{2}$$

$$c_{xx}\dot{x}_1 + c_{xy}\dot{y}_1 + k_{xx}x_1 + k_{xy}y_1 + \frac{k_s}{2}(x_1 - x_2) = 0 \tag{3}$$

$$c_{yx}\dot{x}_1 + c_{yy}\dot{y}_1 + k_{yx}x_1 + k_{yy}y_1 + \frac{k_s}{2}(y_1 - y_2) = 0 \tag{4}$$

where q represents a destabilizing cross-coupled aerodynamic force acting at the rotor center.

It is convenient to nondimensionalize the equations of motion using the following variables

$$X_i = x_i/c \quad , \quad i = 1, 2 \qquad \bar{\delta} = \frac{mg}{ck_s}$$

$$Y_i = y_i/c \quad , \quad i = 1, 2 \qquad Q = \frac{2cq}{mg}$$

$$K_{ij} = \frac{2c}{mg} k_{ij} \quad , \quad i = x, y \qquad \Omega^2 = \omega^2 c/g$$

$$C_{ij} = \frac{2c\omega}{mg} c_{ij} \quad , \quad i = x, y \qquad T = \omega t$$

where c is the bearing radial clearance and ω is the rotor speed. Substitution into equations (1)-(4) yields the following set of nondimensional equations

$$\bar{\delta}\,\Omega^2 X_2'' + (X_2 - X_1) + \frac{\bar{\delta}Q}{2} Y_2 = 0 \tag{5}$$

$$\bar{\delta}\,\Omega^2 Y_2'' + (Y_2 - Y_1) - \frac{\bar{\delta}Q}{2} X_2 = 0 \tag{6}$$

$$C_{xx} X_1' + C_{xy} Y_1' + K_{xx} X_1 + K_{xy} Y_1 + \frac{1}{\bar{\delta}} (X_1 - X_2) = 0 \tag{7}$$

$$C_{yx} X_1' + C_{yy} Y_1' + K_{yx} X_1 + K_{yy} Y_1 + \frac{1}{\bar{\delta}} (Y_1 - Y_2) = 0 \tag{8}$$

where the primes denote differentiation with respect to ωt.

This set of linear ordinary differential equations may be solved to determine the stability of the rotor-bearing system subject to the bearing forces and the equivalent aerodynamic force. The solution to these equations has the form

$$X_i = A_i e^{sT} \quad , \quad i = 1, 2$$

$$Y_i = B_i e^{sT} \quad , \quad i = 1, 2$$

where s represents the system complex eigenvalues,

$$s = P + i\lambda$$

The stability of the system is determined by the sign of P. If $P < 0$, the system is stable and small motions about the system equilibrium position will decay with time. If $P > 0$, the system is pronounced unstable and the motions will increase with time. If $P = 0$, the system is said to be at the onset of instability or instability threshold. It is this condition that will be examined in greater detail. For any given set of conditions, λ represents the rotor whirl ratio, that is, the ratio of the rotating shaft damped natural frequency to the rotor speed.

For any given combination of linearized bearing characteristics and aerodynamic excitation, there is a rotor speed where the real part of the eigenvalue, P, is zero. This rotor speed is the instability onset speed, and the rotor is stable for speeds below this.

Since $P = 0$, by definition, at the instability onset speed, the solution to the equations of motion becomes

$$X_i = A_i e^{i\lambda t} \quad , \quad i = 1, 2 \quad \text{at } \omega = \omega_s$$

$$Y_i = B_i e^{i\lambda t} \quad , \quad i = 1, 2 \quad \text{at } \omega = \omega_s$$

where ω_s is the instability onset speed for the given bearing and aerodynamic conditions. Substitution into equations (4)-(8) gives

$$(1 - \bar{\delta}\,\Omega^2\,\lambda^2)\,X_2 + \frac{\bar{\delta}Q}{2}\,Y_2 - X_1 = 0 \tag{9}$$

$$(1 - \bar{\delta}\,\Omega^2\,\lambda^2)\,Y_2 - \frac{\bar{\delta}Q}{2}\,X_2 - Y_1 = 0 \tag{10}$$

$$(K_{xx} + i\,\lambda\,C_{xx})\,X_1 + (K_{xy} + i\,\lambda\,C_{xy})\,Y_1 + \frac{1}{\bar{\delta}}\,(X_1 - X_2) = 0 \tag{11}$$

$$(K_{yx} + i\,\lambda\,C_{yx})\,X_1 + (K_{yy} + i\,\lambda\,C_{yy})\,Y_1 + \frac{1}{\bar{\delta}}\,(Y_1 - Y_2) = 0 \tag{12}$$

Since equations (9) and (10) are real, they may easily be solved for X_2 and Y_2 in terms of X_1 and Y_1 giving

$$X_2 = \frac{(1 - \bar{\delta}\,\Omega^2\,\lambda^2)\,X_1 - (\bar{\delta}Q/2)\,Y_1}{(1 - \bar{\delta}\,\Omega^2\,\lambda^2)^2 + (\bar{\delta}Q)^2/4} \tag{13}$$

$$Y_2 = \frac{(1 - \bar{\delta}\,\Omega^2\,\lambda^2)\,Y_1 + (\bar{\delta}Q/2)\,X_1}{(1 - \bar{\delta}\,\Omega^2\,\lambda^2)^2 + (\bar{\delta}Q)^2/4} \tag{14}$$

Substitution into equations (11) and (12) gives

$$\left[K_{xx} - \left\{\frac{(\Omega\,\lambda)^2\,(1 - \bar{\delta}\,\Omega^2\,\lambda^2) - \bar{\delta}Q^2/4}{(1 - \bar{\delta}\,\Omega^2\,\lambda^2)^2 + (\bar{\delta}Q)^2/4}\right\} + i\,\lambda\,C_{xx}\right] X_1$$

$$+ \left[K_{xy} + \frac{Q/2}{(1 - \bar{\delta}\,\Omega^2\,\lambda^2)^2 + (\bar{\delta}Q)^2/4} + i\,\lambda\,C_{xy}\right] Y_1 = 0 \tag{15}$$

$$\left[K_{yy} - \left\{\frac{(\Omega\lambda)^2 (1 - \bar{\delta}\Omega^2\lambda^2) - \bar{\delta}Q^2/4}{(1 - \bar{\delta}\Omega^2\lambda^2)^2 + (\bar{\delta}Q)^2/4}\right\} + i\lambda C_{yy}\right] Y_1$$

$$+ \left[K_{yx} - \frac{Q/2}{(1 - \bar{\delta}\Omega^2\lambda^2)^2 + (\bar{\delta}Q)^2/4} + i\lambda C_{yx}\right] X_1 = 0 \qquad (16)$$

A nontrivial solution to this set of equations exists only if the determinant of the matrix of coefficients of X_1 and Y_1 is zero. Since the coefficients are complex, the determinant is also complex. The condition of a zero determinant requires that the real and imaginary parts of the determinant both be zero. Expanding equations (15) and (16) into matrix form and solving for the real and imaginary parts of the determinant results in the following two equations.

$$(K_{xx} - D_1)(K_{yy} - D_1) - (K_{xy} + D_2)(K_{yx} - D_2)$$

$$- \lambda^2 (C_{xx} C_{yy} - C_{xy} C_{yx}) = 0 \qquad (17)$$

$$C_{yy}(K_{xx} - D_1) + C_{xx}(K_{yy} - D_1) - C_{xy}(K_{yx} - D_2)$$

$$- C_{yx}(K_{xy} + D_2) = 0 \qquad (18)$$

where

$$D_1 = \frac{(\Omega\lambda)^2 (1 - \bar{\delta}\Omega^2\lambda^2) - \bar{\delta}Q^2/4}{(1 - \bar{\delta}\Omega^2\lambda^2)^2 + (\bar{\delta}Q)^2/4} \qquad (19)$$

and

$$D_2 = \frac{Q/2}{(1 - \bar{\delta}\Omega^2\lambda^2)^2 + (\bar{\delta}Q)^2/4} \qquad (20)$$

Equations (17) and (18) represent two equations in the two unknows $(\Omega\lambda)^2$ and λ^2. Once these variables are known, the instability onset speed for the given conditions can be determined and is

$$\Omega_s = \frac{(\Omega\lambda)}{\lambda} \tag{21}$$

or in dimensional terms

$$\omega_s = \frac{(\Omega\lambda)}{\lambda}\sqrt{\frac{g}{c}} \tag{22}$$

The solution is obtained in the following way. First, write equation (18) as

$$D_1 = \frac{C_{yy}K_{xx} + C_{xx}K_{yy} - C_{xy}K_{yx} - C_{yx}K_{xy} + D_2(C_{xy} - C_{yx})}{C_{xx} + C_{yy}} \tag{23}$$

For hydrodynamic journal bearings, $C_{xy} = C_{yx}$ (ref. 5) so the last term in equation (23) is zero and D_1 is a function only of the known bearing coefficients,

$$D_1 = \frac{C_{yy}K_{xx} + C_{xx}K_{yy} - C_{xy}K_{yx} - C_{yx}K_{xy}}{C_{xx} + C_{yy}} \tag{24}$$

Once D_1 is known, equation (19) may be solved for $(\Omega\lambda)^2$,

$$(\Omega\lambda)^2 = \frac{(1 + 2\bar{\delta}D_1) \pm \sqrt{(1 + 2\bar{\delta}D_1)^2 - \bar{\delta}(1 + \bar{\delta}D_1)\{\bar{\delta}Q^2(1 + \bar{\delta}D_1) + 4D_1\}}}{2\bar{\delta}(1 + \bar{\delta}D_1)} \tag{25}$$

Now equation (20) is used to determine D_2 and equation (17) is rearranged to give λ^2.

$$\lambda^2 = \frac{(K_{xx} - D_1)(K_{yy} - D_1) - (K_{xy} + D_2)(K_{yx} - D_2)}{C_{xx}C_{yy} - C_{xy}C_{yx}} \tag{26}$$

Finally, equation (21) or (22) is used to determine the instability onset speed. The proper use of equation (25) requires some explanation. If the entire term within the radical is positive, equation (26) gives two real value for $(\Omega\lambda)^2$ and, hence, two instability onset speeds are predicted. For the giv

bearing and aerodynamic conditions, the rotor will be stable only for rotor speeds between the two predicted onset speed values. This condition occurs only for the case when the aerodynamic excitation is greater than zero. As Q approaches zero, the lower value of ω_s approaches zero and the rotor will be stable for all rotor speeds below the upper value of ω_s.

It is apparent from examination of the radical in equation (25) that for a given level of shaft flexibility, δ, and a given set of bearing coefficients, which uniquely determine D_1, there is an upper bound to the level of aerodynamic excitation, Q, that will allow the terms inside the radical to be positive. Once this value of Q is surpassed, the radical term becomes imaginary. This implies that the rotor will be unstable at any rotor speed. Thus, imposing the condition that the radical term be zero in equation (25) will yield the maximum value of aerodynamic excitation for which a stable operating speed exists. Therefore, the maximum aerodynamic excitation the rotor can withstand occurs when

$$(1 + 2\bar{\delta} D_1)^2 - \bar{\delta}(1 + \bar{\delta} D_1)\{\bar{\delta} Q_m^2 (1 + \bar{\delta} D_1) + 4D_1\} = 0 \tag{27}$$

Rearranging gives

$$Q_m = \frac{1}{\bar{\delta}(1 + \bar{\delta} D_1)} \tag{28}$$

Bearing Induced Instability

It is of interest to examine in detail the effect of hydrodynamic bearings alone on the stability of flexible rotors. With aerodynamic excitation Q = 0, equation (19) gives

$$(\Omega\lambda)^2 = \frac{D_1}{1 + \bar{\delta} D_1} \tag{29}$$

where D_1 is calculated from the bearing properties using equation (24). The whirl ratio, λ, is given by equation (26) so the onset speed is

$$\Omega_s = \frac{1}{\lambda}\sqrt{\frac{D_1}{1 + \bar{\delta} D_1}} \tag{30}$$

Noting that with Q = 0, the whirl ratio at the instability onset speed is independent of shaft flexibility, δ, the rigid rotor onset speed is

$$\Omega_{sr} = \frac{1}{\lambda}\sqrt{D_1} \tag{31}$$

so that

$$D_1 = \Omega_{sr}^2 \lambda^2 \tag{32}$$

Substitution into equation (30) gives the flexible rotor instability onset speed as

$$\Omega_s = \frac{\Omega_{sr}}{\sqrt{1 + \bar{\delta}\lambda^2 \Omega_{sr}^2}} \tag{33}$$

which clearly shows the reduction in stability with increasing shaft flexibility. For a given flexibility parameter, $\bar{\delta}$, the rotor instability onset speed can be increased by choosing bearings with a higher bearing instability threshold speed, Ω_{sr}, and lower whirl ratio, λ. As Ω_{sr} becomes very large, the limiting value of instability onset speed becomes

$$\Omega_s = \frac{1}{\lambda\sqrt{\bar{\delta}}} \quad , \quad \Omega_{sr} >> 1 \tag{34}$$

or in dimensional terms

$$\omega_s = \frac{1}{\lambda}\sqrt{\frac{k_s}{m}} \quad , \quad \Omega_{sr} >> 1 \tag{35}$$

Hence the instability onset speed of a flexible rotor is proportional to the rigid bearing natural frequency of the rotor. From equations (24) and (26) it is observed that increased bearing principal stiffness and damping and decreased cross-coupled stiffness increase bearing induced instability onset speeds. Further increases may be obtained from asymmetry in the principal stiffness and damping.

Aerodynamically Induced Instability

If aerodynamic cross-coupling is present it was previously noted that a maximum value of Q exists beyond which a particular flexible rotor-bearing system will be unstable at all speeds. That value was shown to be

$$Q_m = \frac{1}{\bar{\delta}(1 + \bar{\delta} D_1)} \tag{36}$$

With $Q = Q_m$, equation (25) becomes

$$(\Omega\lambda)^2 = \frac{1 + 2\,\bar{\delta}\,D_1}{2\,\bar{\delta}\,(1 + \bar{\delta}\,D_1)} \tag{37}$$

Substituting into equation (20) gives the effective cross coupling at the bearings due to aerodynamic excitation

$$D_2 = \frac{(1 + \bar{\delta}\, D_1)}{\bar{\delta}} \tag{38}$$

This value of D_2 is then used to calculate λ^2.

The instability onset speed becomes

$$\Omega_{sm} = \frac{1}{\lambda}\sqrt{\frac{1 + 2\,\bar{\delta}\, D_1}{2\bar{\delta}(1 + \bar{\delta}\, D_1)}} \tag{39}$$

It should be remembered that equation (38) represents the instability onset speed with maximum aerodynamic cross-coupling present. With smaller values of Q the actual onset speed may be higher or lower as will be subsequently shown.

Example 1 Single-Stage Centrifugal Pump in Plain Cylindrical Journal Bearings. A single-stage centrifugal pump has the impeller centrally mounted on the shaft. The rotor has the following characteristics:

Shaft Length = 107.32 cm
Shaft Diameter = 10.16 cm
Impeller Weight = 1800.0 N
Operating Speed = 4,000 rpm

The rotor is mounted in two identical plain cylindrical journal bearings with the following characteristics:

Bearing Length = 5.08 cm
Bearing Diameter = 10.16 cm
Radial Clearance = 0.0508 mm
Oil Viscosity = 1.23 N-s/cm^2

The shaft weight is 667.2 N. Hence, the modal weight is approximately half the shaft weight plus the impeller weight, or 2134.5 N. The effective shaft stiffness is k_s = 420,283 N/cm which corresponds to δ = 1.0. The bearing coefficients are

$K_{xx} = 2.55$	$C_{xx} = 20.0$
$K_{xy} = 10.0$	$C_{xy} = -2.55$
$K_{yx} = -10.0$	$C_{yx} = -2.55$
$K_{yy} = 1.27$	$C_{yy} = 20.0$

The operating speed parameter is

$$\Omega_0 = \omega_0\sqrt{\frac{c}{g}} = 0.953$$

Equations (24), (36), (38), and (39) give the maximum aerodynamic excitation as

$$Q_m = 0.344$$

and the instability onset speed as

$$\Omega_s = 1.57$$

Since $\Omega_s \neq \Omega_0$, the rotor will be unstable with Q_m present. The variation of instability onset speed with Q is shown by the solid curve in figure 3. This figure was obtained by varying Q is equation (25). The allowable aerodynamic excitation is Q = 0.17. The dashed curve in figure 3 shows the effect of changing the bearing length from 5.08 cm to 4.45 cm which increases the allowable aerodynamic excitation from 0.17 to 0.245.

Optimum Damping

The stability analysis presented in the preceding sections show that for a given set of nondimensional bearing coefficients, the permissible aerodynamic rotor excitation is a function of rotor operating speed and a maximum value is indicated.

The fact that a maximum value of allowable aerodynamic excitation exists may be construed as the existence of an optimum damping. This concept may be visualized in the following way.

Since the nondimensional stiffness and damping coefficients are constant for a given operating condition, increasing the nondimensional speed (the ordinate of stability map) is equivalent to decreasing the dimensional damping in the bearings since damping is inversely proportional to speed. The stability map may be thought of as the effect of increasing the rotor speed assuming the nondimensional bearing stiffness and damping coefficients are independent of speed. The optimum dimensional damping occurs when $\Omega_s = \Omega_{sm}$ and is

$$c_{xx_0} = \frac{W\, C_{xx}}{2c\, \omega_{sm}} \tag{40}$$

$$c_{yy_0} = \frac{W\, C_{yy}}{2c\, \omega_{sm}} \tag{41}$$

where C_{xx} and C_{yy} are the actual nondimensional damping coefficients for the operating conditions being considered and ω_{sm} is the dimensional speed at Ω_{sm}, i.e.,

$$\omega_{sm} = \Omega_{sm} \sqrt{\frac{g}{c}} \tag{42}$$

This value of Ω_s is obviously chosen as the optimum since the maximum allowable aerodynamic excitation, Q_m, occurs at this value. For values of $\Omega_s < \Omega_{sm}$, the actual dimensional damping is excessive, and for $\Omega_s > \Omega_{sm}$, the damping is insufficient. The optimum nondimensional damping coefficients are, therefore,

$$C_{xx_0} = \frac{\omega_0}{\omega_{sm}} C_{xx} \tag{43}$$

$$C_{yy_0} = \frac{\omega_0}{\omega_{sm}} C_{yy} \tag{44}$$

If the bearings or supports are assumed symmetric, an explicit expression for optimum damping may be obtained. Letting

$$K_{xx} = K_{yy} = K_r$$
$$K_{xy} = |K_{yx}| = K_c$$
$$C_{xx} = C_{yy} = C_r$$
$$C_{xy} = C_{yx} << C_r$$

the following relationships are obtained

$$D_1 = K_r$$

$$Q_m = \frac{1}{\bar{\delta}(1 + \bar{\delta}K_r)}$$

$$(\Omega\lambda)^2 = \frac{1 + 2\bar{\delta}K_r}{2\bar{\delta}(1 + \bar{\delta}K_r)}$$

$$\lambda = \frac{1 + \bar{\delta}(K_r + K_c)}{\bar{\delta}C_r}$$

The instability onset speed becomes

$$\Omega_{sm} = \frac{C_r}{1 + \bar{\delta}(K_r + K_c)} \sqrt{\frac{\bar{\delta}(1 + 2\bar{\delta}K_r)}{2(1 + \bar{\delta}K_r)}} \tag{45}$$

For the system to tolerate the maximum aerodynamic excitation, the operating speed must be the same as Ω_{sm},

$$\Omega_0 = \Omega_{sm}$$

and the optimum damping is

$$C_{ro} = \Omega_0 \left\{1 + \bar{\delta}(K_r + K_c)\right\} \sqrt{\frac{2(1 + \bar{\delta}K_r}{\bar{\delta}(1 + 2\bar{\delta}K_r)}} \tag{46}$$

It may be shown (ref.13,14,15) that the effective damping acting at the rotor center is

$$C_e = \left(\frac{2a}{1 + a^2)}\right) C_{em} \tag{47}$$

where a is the ratio of actual bearing damping to optimum bearing damping, i.e.,

$$a = c_r/c_{ro}$$

and C_{em} is the effective damping with optimum bearing damping. Since the allowable aerodynamic is proportional to the effective damping, an estimate of the permissible aerodynamic excitation with non-optimum damping is

$$Q = \left(\frac{2a}{1 + a^2}\right) Q_m \tag{48}$$

Equation (46) can also be written in terms of the bearing (support) principal stiffness to shaft stiffness ratio

$$C_{ro} = \omega_0 \, \omega_{cr} \left(\frac{c}{g}\right) (1 + \bar{\delta}K_c + K) \sqrt{\frac{2(1 + K)}{1 + 2K}} \tag{49}$$

where $K = 2\, k_r/k_s = \bar{\delta}K_r$

Flexible, Damped Bearing Supports

The equations previously presented may also be used to evaluate the effects of squeeze film bearing supports in series with a hydrodynamic bearing. Such a support is shown in figure 4 (ref. 16). In this particular application, the squeeze film is used to support a ball bearing mounted rotor, although any type of shaft bearing may be utilized. The particular values of the squeeze film bearing parameters are, of course, dependent on the rotor-bearing system it will support. The essential features of the squeeze film bearing include an annular clearance between the squeeze film journal and damper housing, lubricant supply grooves or holes, bearing end seals, and journal mechanical retainer springs. Various combinations of these components are used to achieve appropriate stiffness and damping properties for a particular application. Since the squeeze film journal does not rotate, the hydrodynamic squeeze film forces result only from translational motion of the journal which squeezes the lubricant.

Figure 5 schematically illustrates a flexible, damped bearing-support component. The bearing and suppport are represented by general linearized stiff-

ness and damping force coefficients. In many squeeze film bearing applications, the inner bearing mass, m_b, is statically supported in mechanical springs to align and preload the inner bearing within the squeeze film annulus. Therefore, the general support radial stiffness is represented by hydrodynamic stiffness coefficients, k_{0xx} and k_{0yy}, and by the mechanical retainer spring stiffness coefficients, k_{rsx} and k_{rsy}. The bearing and support can be combined to give overall effective stiffness and damping properties (refs. 2, 13). However, care must be exercised when doing so. The effective coefficients are functions of the whirl ratio, λ. Therefore, the use of the stability equations requires an iterative process whereby a value of λ is chosen, the effective coefficients are calculated, and the value of λ predicted by equation (26) is compared with the chosen value. The process is repeated until the calculated and assumed values of λ are the same. A judicious first guess for λ can be made since the damped natural frequency will usually lie somewhere between the undamped natural frequency of the rotor-bearing-support system and the undamped rigid bearing, rigid support natural frequency. Also, the whirl ratio dependence will be much less if either the bearings or supports have a large impedance due to high stiffness or damping.

A further consideration is that under some conditions the effective damping matrix will not be symmetric ($c_{1exy} \neq c_{1eyx}$. With this condition, D_1, given by equation (23), is a function of the aerodynamic cross coupling of the system as well as the bearing coefficients. Equations (20), (23), and (26) must be solved iteratively for D_1 and D_2.

Example 2 11-Stage Centrifugal Compressor

An 11-stage centrifugal compressor is shown in figure 6. The rotor physical characteristics are

Overall Length = 216 cm
Bearing Span = 175.3 cm
Rotor Weight = 5782.4 N
Operating Speed = 10,000 rpm

The first rigid bearing critical speed is N_{cr} = 3894 rpm. The second critical speed is above the 10,000 rpm operating speed with the bearings described above. The rotor is very nearly symmetrical about the bearing midspan and gyroscopic effects are negligible. The rotor modal weight is 2891.2 N, and the shaft stiffness is k_s = 490350 N/cm.

The rotor was originally mounted in tilting pad bearings with the following dimensions:

Length = 5.72 cm
Diameter = 11.43 cm
Radial Pad Clearance = 0.1016 mm
Bearing Radial Clearance = 0.0508 mm
Number of Pads = 5
Pad Arc Length = 60°
Offset Factor = 0.50
Preload = 0.50

Load Direction = Pad Pivot
Oil Viscosity = 1.38×10^{-6} N-s/cm^2

The bearing stiffness and damping coefficients are shown in figure 7 (ref. 7). At 10000 rpm the bearing coefficients are $K_{xx} = K_{yy} = 36.23$, $C_{xx} = C_{yy} = 43.63$. Field experience indicated that the level of aerodynamic excitation at 10000 rpm was q = 35000 N/cm and rotor instability was observed.

Applying equations (36)-(39) the maximum permissible aerodynamic excitation is $Q_m = 0.078$ ($q_m = 11098$ N/cm). This is considerably less than the anticipated value of q = 35000 N/cm. Since Q_m occurs at $\Omega_{sm} = 1.50$ and the operating speed parameter is $\Omega_0 = 3.37$, even less aerodynamic excitation can occur. The variation of Ω_s with Q is shown in figure 8. For $\Omega_s = \Omega_0 = 3.37$, the allowable aerodynamic excitation is Q = 0.055 (q = 7826 N/cm).

If the bearing clearance and pad clearance are increased and pad clearance are increased to 0.1143 mm and 0.2286 mm respectively, the bearing coefficients at 10,000 rpm are

$K_{xx} = 8.83$ $\quad K_{yy} = 14.86$
$C_{xx} = 9.88$ $\quad C_{yy} = 13.29$

For this condition $Q_m = 0.970$ ($q_m = 61340$ N/cm) at $\Omega_{sm} = 1.40$. The operating speed parameter is $\Omega_0 = 5.06$ (the change is due to the change in clearance. The variation of Ω_s with Q for this case is also shown in figure 8. The allowable value of aerodynamic excitation is Q = 0.59 (q = 37310 N/cm). This is slightly larger than the anticipated value. Therefore, it is apparent that large changes in stability can be achieved simply by modifying bearing clearances

CONCLUSIONS

(1) The single mass representation including generalized linearized bearings and aerodynamic excitation yields equations which predict instability onset speeds due to bearing cross coupling and aerodynamic effects.

(2) Expressions for the optimum bearing damping for given bearing stiffness coefficients which will maximize the allowable aerodynamic excitation at a given operating speed and predict the maximum aerodynamic excitation have been developed.

(3) The form of the optimum damping expressions for stability are applicable to first mode synchronous unbalance response and the optimum damping minimizes that response.

(4) Optimum nondimensional bearing damping is a function of the rotr operating speed, rigid bearing undamped critical speed, bearing clearance and ratio of principal bearing stiffness to the fundamental rotor modal.

(5) The effect of flexible, damped bearing supports can be incorporated into the single mass modal representation using equivalent bearing-support linear stiffness and damping coefficients.

REFERENCES

1. Abdul-Wahed, Frene, J., and Nicolas, D., "Analysis of Fitted Partial Arc and Tilting Pad Journal Bearings," Trans. ASLE, Paper No. 78-AM-2A-3.

2. Warner, R. E. and Soler, A. I., "Stability of Rotor-Bearing Systems with Generalized Support Flexibility and Damping and Aerodynamic Cross-Coupling," Trans. ASME, Journal of Lubrication Technology, July 1975, pp. 461-471.

3. Lund, J. W., "The Stability of an Elastic Rotor in Journal Bearings with Flexible Damped Supports," Trans. ASME, Journal of Applied Mechanics, Vol. 87, 1965, pp. 911-920.

4. Lund, J. W., "Spring and Damping Coefficients for the Tilting Pad Journal Bearing," Trans. ASLE, Vol. 7, No. 4, 1964, pp. 342-352.

5. Lund, J. W. and Thomsen, K. K., "A Calculation Method and Data for the Dynamic Coefficients of Oil-Lubrication Journal Bearings," Topics in Fluid Film Bearing and Rotor Bearing System Design and Optimization, April 1978, pp. 1-28.

6. Nicholas, J. C., "A Finite Element Analysis of Pressure Dam and Tilting Pad Bearings," Ph.D. Dissertation, University of Virginia, May 1977.

7. Nicholas, J. C., Gunter, E. J., and Allaire, P. E., "Stiffness and Damping Coefficients for the Five-Pad Tilting-Pad Bearing," Trans. ASLE, Paper No. 77-LC-3A-2, 1977.

8. Hagg, A. C. and Sankey, G. O., "Elastic and Damping Properties of Oil-Film Journal Bearings for Applicat to Unbalance Vibration Calculations, Trans. ASME, Journal of Applied Mechanics, March 1958, pp. 141-143.

9. Li, D. F., Allaire, P. E., and Barrett, L. E., "Analytical Dynamics of Partial Journal Bearings with Applications," Trans. ASLE, Paper No. 77-LC-1A-1, 1977.

10. Alford, J. S., "Protecting Turbomachinery from Self-Excited Rotor Whirl," Trans. ASME, Journal of Engineering for Power, Oct. 1965, pp. 333-344.

11. Gunter, E. J., Barrett, L. E., and Allaire, P. E., "Stabilization of Turbomachinery with Squeeze Film Dampers - Theory and Application," I. Mech. E., Proceedings of Conference on Vibrations in Rotating Machinery, Cambridge, England, C233/76, Sept. 1976.

12. Lund, J. W., "Stability and Damped Critical Speeds of a Flexible Rotor in Fluid Film Bearings," Trans. ASME, Journal of Engineering for Industry, Vol. 96, 1974, pp. 509-517.

13. Barrett, L. E., "Stability and Nonlinear Response of Rotor-Bearing Systems with Squeeze Film Bearings," Ph.D. Dissertation, University of Virginia, August 1978.

14. Barrett, L. E., Gunter, E. J., and Alliare, P. E., "Optimum Bearing and Support Damping for Unbalance Response and Stability of Turbomachinery," Trans. ASME, Journal of Engineering for Power, Jan. 1978, pp. 89-94.

15. Black, H. F., "Stabilizing Capacity of Bearings for Flexible Rotors with Hysteresis," Trans. ASME, Journal of Engineering for Industry, Feb. 1976, pp. 87-91.

16. Cunningham, R. E., Fleming, D. P., and Gunter, E. J., "Design of a Squeeze Film Damper for a Multimass Flexible Rotor," Trans. ASME, Journal of Engineering for Industry, 1976.

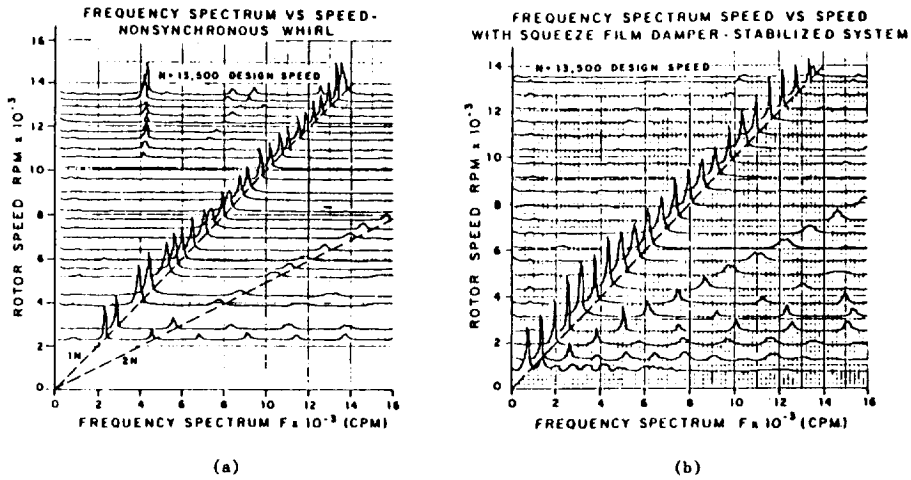

Fig. 1. Frequency Spectra of 7-Stage Centrifugal Compressor
(a) Subsynchronous Instability with N > 10500 RPM
(b) Stabilization with Well Designed Squeeze Film Bearing

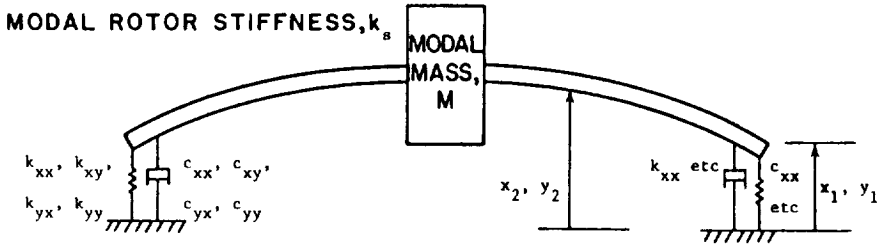

Fig. 2 Schematic of Single Mass Representation of Symmetric Multimass Rotors

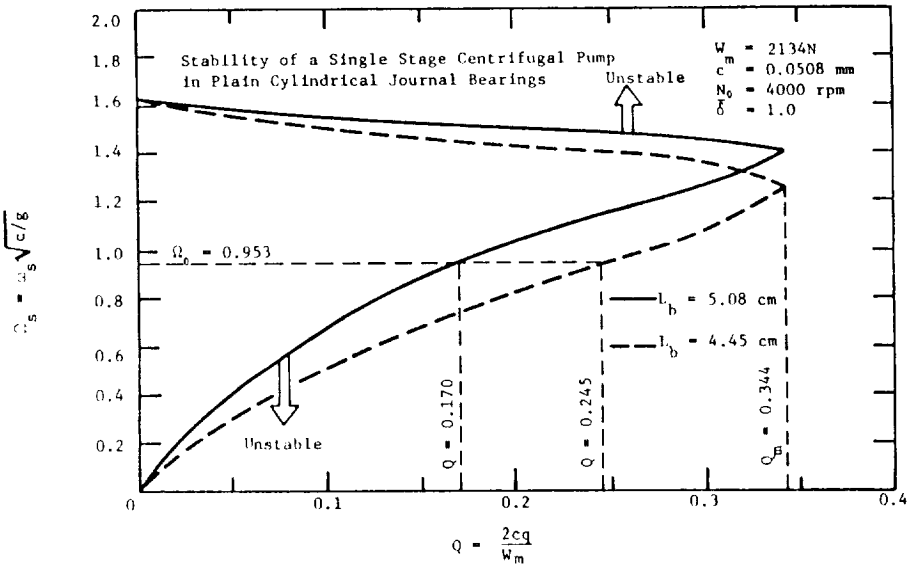

Fig. 3.

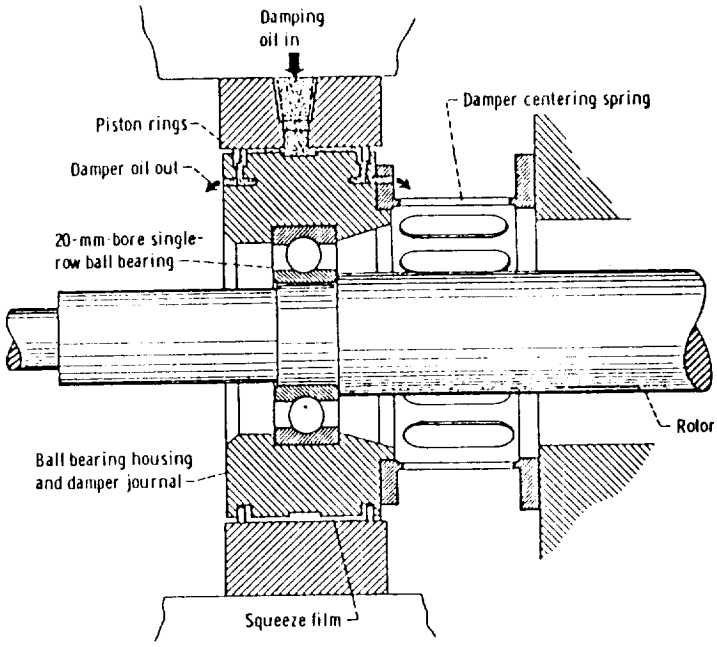

Fig. 4 Axial Cross Section of Squeeze Film Bearing Used in NASA Experimental Work. Ref (Cunningham, 1977)

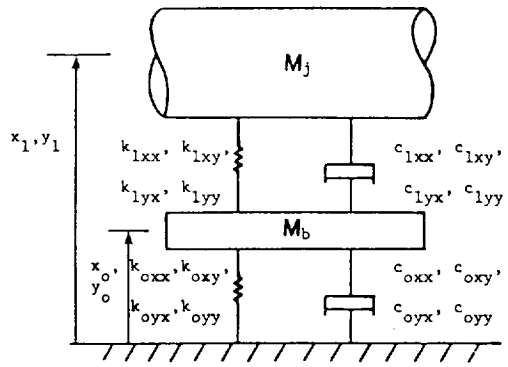

Fig. 5. Schematic of Bearing in Flexible, Damped Supports

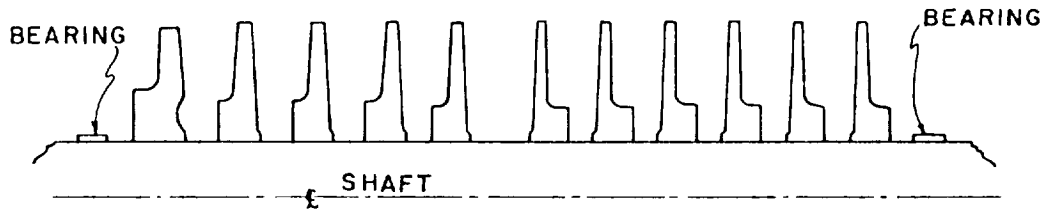

Fig. 6 - Schematic of 11-Stage Centrifugal Compressor

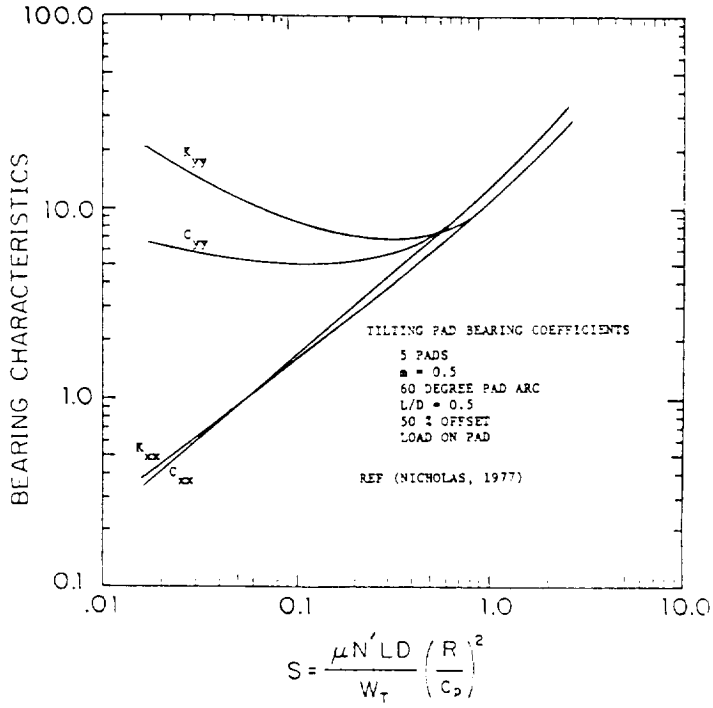
100.0
10.0
1.0
0.1
.01
0.1
1.0
10.0
BEARING CHARACTERISTICS
K_{yy}
C_{yy}
K_{xx}
C_{xx}
TILTING PAD BEARING COEFFICIENTS
5 PADS
m = 0.5
60 DEGREE PAD ARC
L/D = 0.5
50 % OFFSET
LOAD ON PAD
REF (NICHOLAS, 1977)
$S = \frac{\mu N' LD}{W_T}\left(\frac{R}{c_p}\right)^2$

Fig. 7

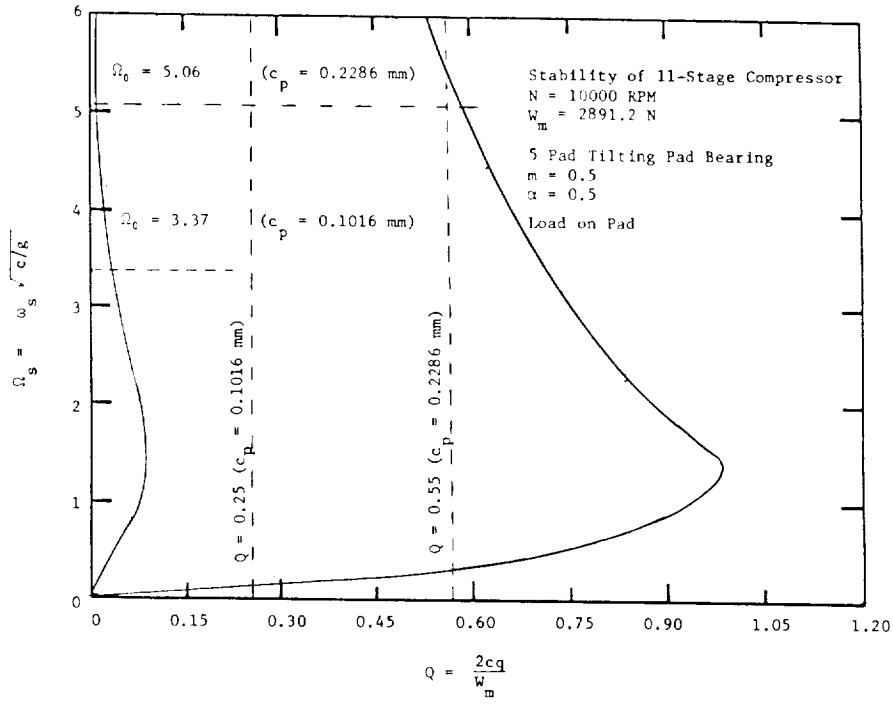
Ω_0 = 5.06
(c_p = 0.2286 mm)
Ω_c = 3.37
(c_p = 0.1016 mm)
Stability of 11-Stage Compressor
N = 10000 RPM
W_m = 2891.2 N
5 Pad Tilting Pad Bearing
m = 0.5
α = 0.5
Load on Pad
Q = 0.25 (c_p = 0.1016 mm)
Q = 0.55 (c_p = 0.2286 mm)
$\Omega = \omega_s \sqrt{c/g}$
0
1
2
3
4
5
6
0
0.15
0.30
0.45
0.60
0.75
0.90
1.05
1.20
$Q = \frac{2cq}{W_m}$

Fig. 8